Available online at www.sciencedirect.com

ScienceDirect

Procedia Materials Science 7 (2014) 38 – 52

Procedia Materials Science

www.elsevier.com/locate/procedia

2nd International Summer School on Nuclear Glass Wasteform: Structure, Properties and Long-Term Behavior, SumGLASS 2013

Building Monte Carlo models of glasses using neutron and/or X-ray diffraction data

D.T. Bowron

ISIS Pulsed Neutron and Muon Source, STFC Rutherford Appleton Laboratory, Chilton, Didcot, OX11 0QX, United Kingdom

Abstract

Neutron and X-ray diffraction are key techniques that are used to investigate the atomic and nanometric mesoscale structure of glasses and amorphous materials. These experimental methods probe the nuclear (neutron) or atomic (X-ray) pair correlation functions between atoms. For a multicomponent glass containing N atom types, the information content of the data is low, considering that the data are a weighted sum of N(N+1)/2 partial pair correlation terms. This complexity can often make direct interpretation of results difficult or impossible. Modern computational methods can now rapidly refine atomistic models of disordered materials that satisfy the constraints imposed by diffraction data. These models can then be used to investigate how the partial pair correlation functions contribute to the total scattering data, given a chosen set of underlying physico-chemical constraints, and allow us to extract many structural functions of interest such as bond angle distributions and coordination number histograms. To illustrate these capabilities the technique of Empirical Potential Structure Refinement (EPSR), has been applied to a range of results from a selection of oxide-glass systems and the results provide a set of reference parameters that can be used in future studies on similar glass systems where EPSR is the goal.

Selection and peer-review under responsibility of the scientific committee of SumGLASS 2013

Keywords: Glass Structure; Neutron Diffraction; X-ray Diffraction; Empirical Potential Structure Refinement

PACS: 61.43.Fs, 61.05.fg, 61.05.cf, 61.43.Bn

1. Introduction

The lack of long range order and periodicity in the configurations of atoms and molecules that make up amorphous materials poses a number of quite significant challenges for the glass scientist. This is because the primary tool used for the characterisation of materials structure, the crystallographic method, cannot be applied to deliver the standard information about symmetry, unit cell and space group, that generally forms the basis of the physico-chemical understanding of a material's properties. To make progress with glasses and other amorphous systems, attention must instead be turned to concepts of short-range atomic structure such as local chemical order, local symmetry and

* D.T. Bowron. Tel.: +44-1235-446381 ; fax: +44-1235-445720.
E-mail address: daniel.bowron@stfc.ac.uk (D.T. Bowron).

Selection and peer-review under responsibility of the scientific committee of SumGLASS 2013
doi:10.1016/j.mspro.2014.10.007

statistical distribution functions that characterise the envelope of structural correlations in the disordered network, Zallen (1983).

Although crystallographic approaches are unsuitable for addressing questions of glass structure, neutron and X-ray diffraction are still arguably the most direct probes of many of the structural issues of interest, albeit that the information is contained in the diffuse scattering patterns that are measured, rather than in sharp Bragg features. In effect these scattering experiments probe the pair correlations between atoms in the material reflecting the radial distribution function of atomic centres, instead of the single particle correlation function that characterises a periodic crystalline lattice, Lovesey (1984).

In spite of the power of the diffraction techniques for looking at non-crystalline systems, there does remain one particular difficulty. This is the fact that for any given radial distribution function, there are an infinite number of higher body arrangements of atoms, characterised through the three-body, four-body etc. distribution functions, with which it would be compatible, Cusack (1987). For example this means that if we build an atomistic model of an amorphous material that is consistent with the radial distribution function measured in a diffraction measurement, this structure will not be unique and more information will be required if the veracity of the model is to be established. This does not mean that the diffraction experiment is useless, since it is still an essential criterion that any successful model of a glassy system must reproduce the experimentally observed pair distribution function, and any model that does not do this is clearly incorrect.

Thankfully the extra information required to build a robust model of a glass is often simple to derive from physico-chemical knowledge. This includes knowledge about the relative sizes of atoms, the density of the material, the bonding capabilities of atoms and the structure of molecular or pseudo-molecular units. Taken collectively, this information provides some stringent constraints on the distributions of atomic positions and the local higher-body correlations that can be considered to occur in a non-crystalline network, and we will show how the combination of diffraction and constrained computer modelling can now deliver considerable insight into the structure of glassy materials.

2. Theory

In a neutron or X-ray diffraction experiment that is performed on a liquid or glassy system, the structural function that is measured is the interference differential scattering cross section or total structure factor, $F(Q)$, where Q is the magnitude of the momentum transfer vector of the scattering process,

$$Q = \frac{4\pi}{\lambda}\sin\theta \tag{1}$$

λ is the wavelength of the incident radiation, and 2θ is the scattering angle. For neutron diffraction $F(Q)$ is defined as,

$$F(Q) = \sum_{\alpha\leq\beta}(2-\delta_{\alpha\beta})c_\alpha c_\beta\langle b_\alpha\rangle\langle b_\beta\rangle[S_{\alpha\beta}(Q)-1] \tag{2}$$

c_α, c_β, $\langle b_\alpha\rangle$ and $\langle b_\beta\rangle$ are the atomic fractions and bound coherent neutron scattering lengths (averaged over nuclear spin and isotope states), Sears (1992) of atoms of type α and β respectively, and $S_{\alpha\beta}(Q)$ are the partial structure factors that encode the correlations between pairs of atoms in reciprocal space that make up the total structure factor. $\delta_{\alpha\beta}$ is the Kronecker δ function to avoid double counting correlations between atoms of the same type. For comparison, in an X-ray diffraction experiment $F(Q)$ is formulated as,

$$F(Q) = \sum_{\alpha\leq\beta}(2-\delta_{\alpha\beta})c_\alpha c_\beta f_\alpha(Q)f_\beta(Q)[S_{\alpha\beta}(Q)-1] \tag{3}$$

where the bound coherent scattering lengths of the neutron diffraction experiment are replaced with $f_\alpha(Q)$ and $f_\beta(Q)$, the Q-dependent atomic form factors for atoms of type α and β, Waasmaier and Kirfel (1995). This difference highlights an important complementarity between neutron and X-ray diffraction measurements, the neutron experiment probes the pair correlations between atomic nuclei, whilst the X-ray diffraction measurement probes the correlations between the atoms through their bound electron distributions.

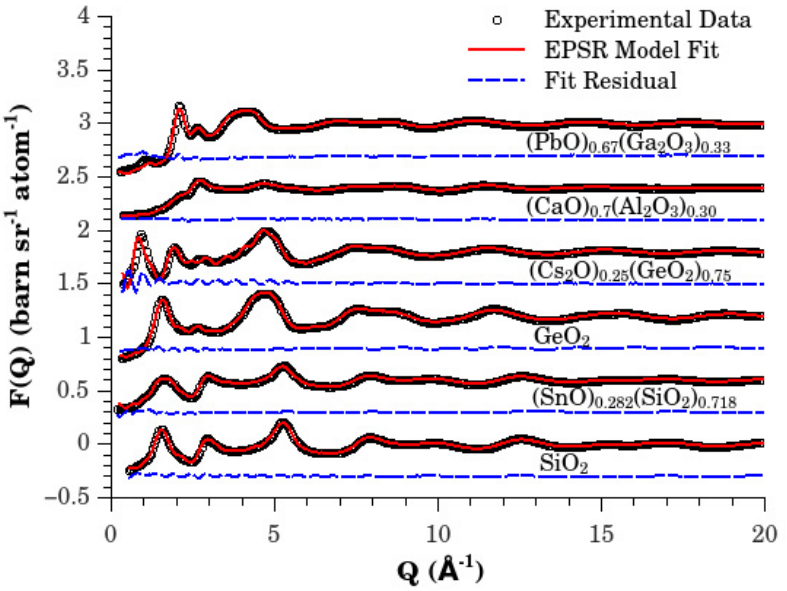

Fig. 1. The EPSR model fits (red solid line) and fit residuals (blue dotted line) to the experimental $F(Q)$ measured for SiO_2, Bowron (2008a), $(SnO)_{0.282}(SiO_2)_{0.718}$, Bent et al. (1998), GeO_2, Hannon et al. (1990), $(Cs_2O)_{0.25}(GeO_2)_{0.75}$, Hannon et al. (2007), $(CaO)_{0.70}(Al_2O_3)_{0.30}$, Hannon and Parker (2000) and $(PbO)_{0.67}(Ga_2O_3)_{0.33}$, Hannon et al. (1998) glasses. The experimental data are shown as black circles and for clarity are vertically offset by 0.0, 0.6, 1.2, 1.8, 2.4 and 3.0 units, respectively. The corresponding fit residuals are vertically offset by -0.3, 0.3, 0.9, 2.1 and 2.7 units.

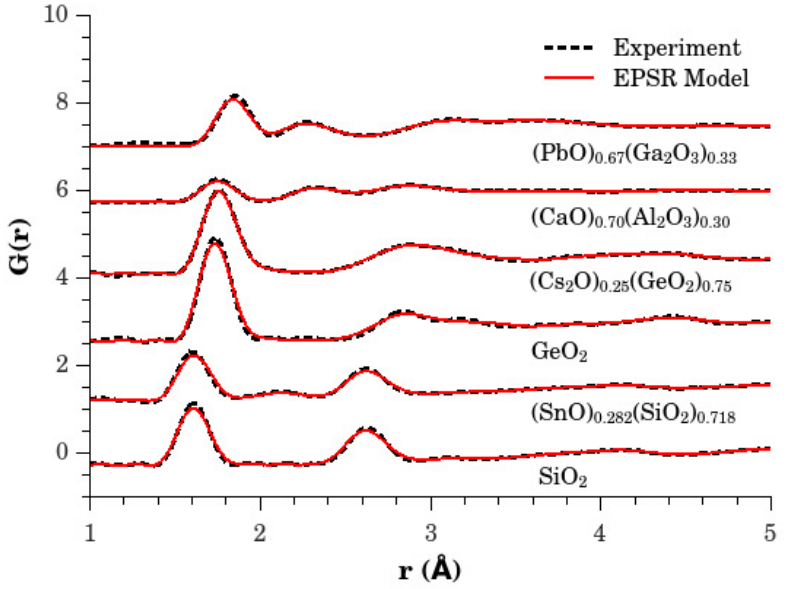

Fig. 2. The total radial distribution functions, $G(r)$, of the experimental data (black dotted lines) and EPSR model fits (red solid lines) of SiO_2, Bowron (2008a), $(SnO)_{0.282}(SiO_2)_{0.718}$, Bent et al. (1998), GeO_2, Hannon et al. (1990), $(Cs_2O)_{0.25}(GeO_2)_{0.75}$, Hannon et al. (2007), $(CaO)_{0.70}(Al_2O_3)_{0.30}$, Hannon and Parker (2000) and $(PbO)_{0.67}(Ga_2O_3)_{0.33}$, Hannon et al. (1998) glasses. The experimental data and model functions are offset by 0.0, 1.5, 3.0, 4.5, 6.0 and 7.5 units respectively.

The total structure factor is related to the total radial distribution function $G(r)$ by a Fourier transform,

$$G(r) = \frac{1}{(2\pi)^3\rho_0}\int_0^\infty 4\pi Q^2 F(Q)\frac{\sin Qr}{Qr}dQ \tag{4}$$

weighted by the average number density of the material, ρ_0, in atoms Å^{-3}. In similar fashion to Equations 2 and 3, the total radial distribution is formed from a weighted sum of the partial pair distribution functions $g_{\alpha\beta}(r)$ as,

$$G(r) = \sum_{\alpha\leq\beta}(2-\delta_{\alpha\beta})c_\alpha c_\beta\langle b_\alpha\rangle\langle b_\beta\rangle[g_{\alpha\beta}(r)-1] \tag{5}$$

In a neutron diffraction experiment this definition of the total radial distribution function leads to some fundamental limiting values for the behaviour of $G(r)$ at very short and very long distances, that can be useful in checking the reliability of experimental scattering data and model predictions. These limiting values are given by, Keen (2001):

$$G(r<r_0) = -\textstyle\sum_\alpha (c_\alpha\langle b_\alpha\rangle)^2 \;\; G(r\rightarrow\infty) = 0 \tag{6}$$

where r_0 is the shortest interatomic pair distance in the system.

Each partial pair distribution function in Equation 5 is explicitly defined in terms of the number of particles of type β found in a radial shell between distances of r and $r+dr$ from a particle of type α ($n_{\alpha\beta}(r)$) by,

$$g_{\alpha\beta}(r) = \frac{n_{\alpha\beta}(r)}{4\pi\rho_\beta r^2 dr} \tag{7}$$

where $\rho_\beta = c_\beta\rho_0$. This relationship consequently allows us to define the coordination number for the number of atoms of type β found about atoms of type α in a radial shell delimited by inner and outer shell distances, r_1 and r_2, as:

$$\left(N_\beta^{(\alpha)}\right)_{r_1}^{r_2} = 4\pi\rho_\beta\int_{r_1}^{r_2} r^2 g_{\alpha\beta}(r)dr \tag{8}$$

This quantity, along with the most probable atomic pair distances given by the positions of the peaks in $G(r)$ or $g_{\alpha\beta}(r)$, is frequently seen as one of the key pieces of information required of any comprehensive characterisation of a glass structure. In atomistic structural analyses the coordination number is often plotted as a running sum, $N(r)$, evaluated outwards from an origin atom over shells of increasing radius r. It is also worth pointing out the symmetry in the partial pair distribution functions i.e. $g_{\alpha\beta}(r) = g_{\beta\alpha}(r)$, but note that this symmetry does not apply to the coordination numbers which will differ in proportion to $c_\alpha\rho_0$ and $c_\beta\rho_0$.

Considering the permutations of atom pairs that contribute to Equation 5 for a sample containing N atom types, there will be $N(N+1)/2$ partial pair distribution functions to take into account when interpretting the total radial distribution function. This highlights an additional difficulty that contributes to the aforementioned issue of the uniqueness of any structural model based on a pair distribution function, that must also be faced by the experimental scientist trying to understand the structure of a multicomponent amorphous material. A single neutron or X-ray diffraction experiment will only allow the determination of the total radial distribution function as there is insufficient information in the measured signal to permit the separation of the function into the partial pair distributions that are often of primary interest to the materials scientist. In the following section we will discuss a computational strategy to help with this problem.

3. Modelling

From an experimental perspective, methods have been developed over the past few decades to help address the challenge of unfolding the contributions of the partial pair distribution terms to the total radial distribution function. In particular these include neutron diffraction with isotopic substitution, Enderby et al. (1966), anomalous X-ray scattering, Fuoss et al. (1981), and multi-technique approaches, Bowron (2008b); Fischer et al. (2006). In each case the aim is to capitalize on complementary viewpoints on the total radial distribution functions, obtained by varying the scattering power of selected elements or by using different structure probing experimental techniques, to permit enhanced understanding of the relative contributions of the partial pair terms to the total. Although these methods

sometimes allow us to directly access specific partial pair distribution functions of interest, in most real-world cases the compositional complexities of the materials of interest are too great for a complete separation of the contributing functions by experiments alone. In these cases, it is generally necessary to adopt brute force computational strategies in which *a priori* information about chemical behaviour and physical properties can be used to guide the generation of atomistic models that are consistent with available diffraction data. Once a model exists, all the partial pair distribution functions are accessible, and tests can be performed on how sensitive the results are to assumed information that was used to guide the model generation.

One such method that is finding increasing utility in this area is Empirical Potential Structure Refinement (EPSR), that was developed by Soper (1996, 2005, 2011b). The approach uses a classical, NVT, Monte Carlo simulation (Allen and Tildesley (1987)) combined with perturbation potentials derived from experimental data, to setup a distribution of atoms and molecules that is consistent with the structure factors measured in a neutron or X-ray diffraction experiment. The simulation as a whole is driven by potential energy functions operating between pairs of atoms separated by a distance r, that can be split into two terms, a reference potential $U_{\alpha\beta}^{(Ref)}(r)$ and an empirically derived perturbation potential $U_{\alpha\beta}^{(EP)}(r)$,

$$U_{\alpha\beta}(r) = U_{\alpha\beta}^{(Ref)}(r) + U_{\alpha\beta}^{(EP)}(r) \tag{9}$$

In general the reference potential takes the standard form of a Lennard-Jones 12-6 potential, plus Coulomb charges where appropriate, i.e.

$$U_{\alpha\beta}^{(Ref)}(r) = 4\epsilon_{\alpha\beta}\left[\left(\frac{\sigma_{\alpha\beta}}{r}\right)^{12} - \left(\frac{\sigma_{\alpha\beta}}{r}\right)^{6}\right] + \frac{q_\alpha q_\beta}{4\pi\epsilon_0 r} \tag{10}$$

For unlike atomic species the values of $\epsilon_{\alpha\beta}$ and $\sigma_{\alpha\beta}$ are generated using the Lorentz-Berthelot mixing rules on the values for the individual atomic components, Allen and Tildesley (1987),

$$\epsilon_{\alpha\beta} = (\epsilon_\alpha \epsilon_\beta)^{\frac{1}{2}} \;\; \sigma_{\alpha\beta} = \tfrac{1}{2}(\sigma_\alpha + \sigma_\beta) \tag{11}$$

In contrast to the reference potential the empirical perturbation potentials have more complex forms as they are derived from differences between the structure factors calculated from the model of the atomic configurations of the material under study, and those measured in a neutron or X-ray diffraction experiment, see Soper (2005) for more details. Ideally, if the reference potential is well chosen, the Monte Carlo simulation will produce a reasonable estimate of the structure of the system of interest without the application of the empirical potential, and only small adjustments to the interatomic interaction potentials will then be needed to bring the structural configurations into optimal agreement with the experimental data.

Equation 10 shows us how key physico-chemical information can be incorporated into the model from the outset, to make up for some of the deficiencies in the information content of the scattering data. For atomic glasses, key parameters are the sizes of the atomic components that are encoded in the values of σ, and chemical bonding and valence preferences which can be included through the use of Coulomb charges, q. The density of the system being modelled is fixed through the use of the NVT ensemble and lastly, if the system of interest were formed from molecular units, the short range atomic connectivity of the molecules is also maintained throughout the modelling process, although each molecule is periodically disordered to account for the unavoidable quantum zero-point disorder that is reflected in the measured distributions of intra-molecular bond lengths.

If the data is available, the model can be refined against multiple data sets from isotopic substitution neutron scattering series or combinations of neutron and X-ray scattering measurements. These multi-data refinements are often useful to impose additional constraints on the models that are produced.

The structure refinement method is then implemented to the following recipe:

1. Prepare neutron and/or X-ray scattering structure factor data for refinement. Data should be corrected for experimental factors such as absorption, multiple scattering, container and instrument background contributions, inelasticity or Compton scattering etc. The structure factor should also be normalized to a known scheme, Soper (2011c).
2. Using an appropriate set of reference potential parameters, build an atomistic representation of the material taking care to maintain the chemical stoichiometry of the model, the atomic density and charge balance of the system.

Table 1. Lennard-Jones and charge parameters used for the references potentials to model SiO_2, Bowron (2008a), $(SnO)_{0.282}(SiO_2)_{0.718}$, Bent et al. (1998), GeO_2, Hannon et al. (1990), $(Cs_2O)_{0.25}(GeO_2)_{0.75}$, Hannon et al. (2007), $(CaO)_{0.70}(Al_2O_3)_{0.30}$, Hannon and Parker (2000) and $(PbO)_{0.67}(Ga_2O_3)_{0.33}$, Hannon et al. (1998) glasses. Note that the coulomb charges used to constrain the local chemical order in the glass network were scaled down by a factor of 2 to increase the speed of the Monte Carlo engine for driving the atomic configurations into agreement with the experimental structure factors and reduce the need for generating large empirical perturbation potentials.

Atom	ϵ [kJ/mol]	σ [Å]	q [e]	Mass [amu]
O	0.1625	3.600	-1.0000	16.0
Al	0.1750	1.330	1.5000	27.0
Si	0.1750	1.030	2.0000	28.1
Ca	0.1750	2.630	1.0000	40.1
Ga	0.1750	1.600	1.5000	69.7
Ge	0.2000	1.410	2.0000	72.6
Sn	0.0075	1.000	0.5000	118.7
Cs	0.2000	4.350	0.5000	132.9
Pb	0.2000	2.400	1.0000	207.2

3. Calculate the appropriate scattering weights (c_i, $\langle b_i \rangle$ and/or c_i, $f_i(Q)$ products) that link the model to the experimental data.
4. Equilibrate the model using the Monte Carlo simulation engine operating on the reference potential parameters alone.
5. Once the structure has equilibrated to atomic configurations consistent with the reference potential, turn on the feedback mechanism that estimates an empirical perturbation potential from the difference between calculated and experimental structure factors, then continue to run the Monte Carlo engine until agreement is reached between the model and experimental data.
6. Start accumulating ensemble average information on parameters of interest in the model such as partial pair distribution functions, bond angle distribution functions, coordination number histograms etc.

It is important to remember that the only goal of the EPSR procedure is the production of an ensemble of atomic configurations that is consistent with the nuclear (neutron) or atomic (X-ray) pair correlation functions measured in diffraction experiments. This is just *a model*. The configurations are simply lists of atomic coordinates that are distributed according to the constraints imposed by the experimental data, and the assumed parameters governing the density of the material, the relative sizes of the atoms, and the local chemical stoichiometry that can be controlled through the use of Coulomb charges to encode valence and ionic/covalent bonding preferences. The precise form of the potential energy terms that underly the operational mechanics of the modelling engine are relatively unimportant, since their only purpose is to provide an efficient means by which sensible atomic configurations can be generated and sampled. There is one caveat to this statement, in that the reference potentials must not exclude required atomic correlations from the model, such as through the definition of over-large atomic radii which would prevent atoms adopting appropriate first neighbour distances. Although in theory the empirical potential could evolve to counter this constraint, in practice this would not happen reliably as the method works best when operating under mild perturbative conditions. Once an ensemble of structures matches the constraints imposed by the experimental data, it is then the responsibility of the investigating scientist to decide if the structural conclusions that can be drawn from the model, are reasonable or otherwise. This usually requires reference to independent results that were not explicitly incorporated in the constraints used to define the model generation. If the model highlights an unexpected conclusion, then further models can be generated where constraints are added to either explicitly exclude or impose a structural feature under question, and in this way we can test hypotheses for compatibility with the diffraction data using the EPSR modelling engine.

4. Examples of application

To demonstrate the utility of the method for extracting structural information from diffraction data, we have constructed a series of models of some standard glass forming systems for which high quality neutron scattering data

Table 2. The composition, box size and density parameters used to model SiO_2, Bowron (2008a), $(SnO)_{0.282}(SiO_2)_{0.718}$, Bent et al. (1998), GeO_2, Hannon et al. (1990), $(Cs_2O)_{0.25}(GeO_2)_{0.75}$, Hannon et al. (2007), $(CaO)_{0.70}(Al_2O_3)_{0.30}$, Hannon and Parker (2000) and $(PbO)_{0.67}(Ga_2O_3)_{0.33}$, Hannon et al. (1998) glasses.

Glass	Atomic components & number in box	Side length of simulation box [Å]	Density [atoms Å^{-3}]
SiO_2	Si 500	28.3	0.0664
	O 1000		
$(SnO)_{0.282}(SiO_2)_{0.718}$	Sn 282	35.1	0.0635
	Si 718		
	Al 12		
	O 1736		
GeO_2	Ge 500	28.8	0.0629
	O 1000		
$(Cs_2O)_{0.25}(GeO_2)_{0.75}$	Cs 250	30.6	0.0523
	Ge 375		
	O 875		
$(CaO)_{0.70}(Al_2O_3)_{0.30}$	Ca 420	28.8	0.0732
	Al 360		
	O 960		
$(PbO)_{0.67}(Ga_2O_3)_{0.33}$	Pb 335	28.7	0.0632
	Ga 330		
	O 830		

is available. Specifically models of glassy SiO_2, Bowron (2008a), $(SnO)_{0.282}(SiO_2)_{0.718}$, Bent et al. (1998), GeO_2, Hannon et al. (1990), $(Cs_2O)_{0.25}(GeO_2)_{0.75}$, Hannon et al. (2007), $(CaO)_{0.70}(Al_2O_3)_{0.30}$, Hannon and Parker (2000) and $(PbO)_{0.67}(Ga_2O_3)_{0.33}$, Hannon et al. (1998) have been generated, and where the series presents the opportunity to provide model reference potential parameters for nine elements that are commonly found in glass forming systems. These parameters are summarized in Table 1 whilst the composition, model size and density parameters for each specific glass model are summarized in Table 2.

Figures 1 and 2 show the EPSR fits to the measured total structure factors and corresponding total radial distribution functions of each glass, demonstrating the typical levels of agreement that can be obtained between model and experiment. Each of the total radial distribution functions shown in Figure 2 contains contributions from three or six partial pair terms depending on whether it is from a two component or three component glass. This limits our ability to unambiguously assign structural correlations to only the nearest neighbour features such as the $Si-O$ bonds at 1.60Å, the $Ge-O$ bonds at 1.72Å, and the $Al-O$ and $Ga-O$ bonds at 1.73Å and 1.83Å respectively. As one moves to larger distances the chances of overlapping correlations contributing to the same region of $G(r)$ increases markedly such that beyond 3Å the task of simple peak assignment becomes impossible. For reference, the limits of the direct analysis of $G(r)$ for the three component glasses discussed here, have been shown in references, Bent et al. (1998); Hannon et al. (2007); Hannon and Parker (2000); Hannon et al. (1998).

4.1. Network forming partial structure factors

In respect to this issue, the advantage of analytical approaches such as EPSR can immediately be illustrated. Figures 3, 4 and 5 show the partial pair distribution functions for the glass network forming components, Si, Ge, Al, Ga and O that are consistent with the measured total structure factors of Figure 1, and the physico-chemical constraints imposed by the reference potential parameters and the density of the systems. In particular one notes, that the method allows us to easily estimate more distant pair correlations, > 3Å, that are consistent with the local chemical order, and also evalute the number of atoms and extent of disorder involved in the intermediate range order in the materials.

If we take the pure SiO_2 and GeO_2 systems as the archetypical examples of glass forming systems, these models clearly highlight four-fold coordination of the Si and Ge atoms by O in their first coordination shell of the $Si-O$ and

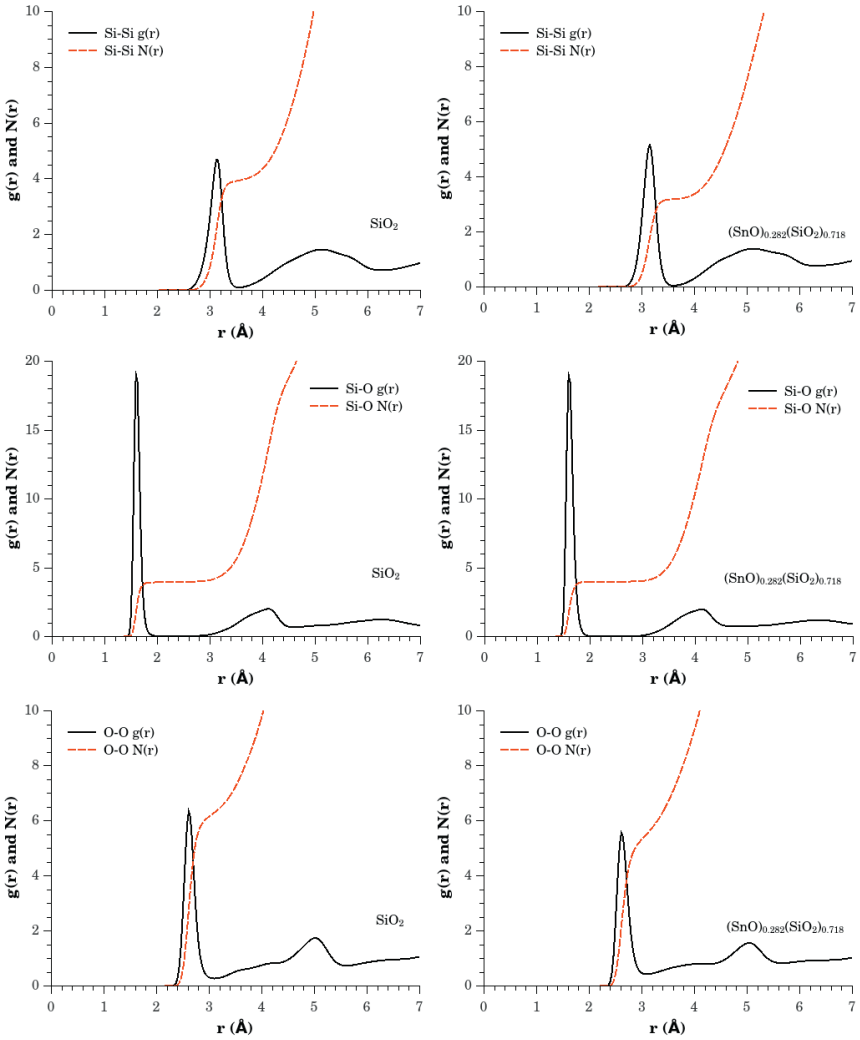

Fig. 3. The partial pair distribution functions (black solid lines) and running coordination numbers (red broken lines) for the network forming components of SiO_2 and $(SnO)_{0.282}(SiO_2)_{0.718}$ glasses.

$Ge-O$ partial distribution functions, and show that this local ordering persists to the second shell with each O atom briding to another Si or Ge atom, leading to four fold coordination in the first peak of the $Si-Si$ and $Ge-Ge$ partial distribution functions. The $O-O$ partial distribution functions do however highlight some subtle differences between the SiO_2 and GeO_2 glass networks. In the SiO_2 system each O atom is coordinated by ≈ 6 neighbouring O atoms in its second shell, whilst in GeO_2 this value is found to be closer to ≈ 8 neighbouring O atoms, the first shell being formed from 4 Si or 4 Ge atoms.

The affect of the addition of the network modifier atoms Sn and Cs to the SiO_2 and GeO_2 glass networks can now also be appreciated through the $Si-O$, $Ge-O$, $Si-Si$, $Ge-Ge$ and $O-O$ partial pair distribution functions. In both the silicate and germanate glass systems investigated, the addition of the network modifier does not change the preference for four-fold coordination of the Si or Ge atoms by O in their first coordination shell, but in the second neighbour region for Si in the $(SnO)_{0.282}(SiO_2)_{0.718}$ glass, the Sn atoms are seen to compete with the Si atoms for a presence in this second shell, manifest through a reduction in $\left(N_{Si}^{(Si)}\right)_{2.5}^{3.6}$ from ~ 4 to ~ 3. This does not appear to

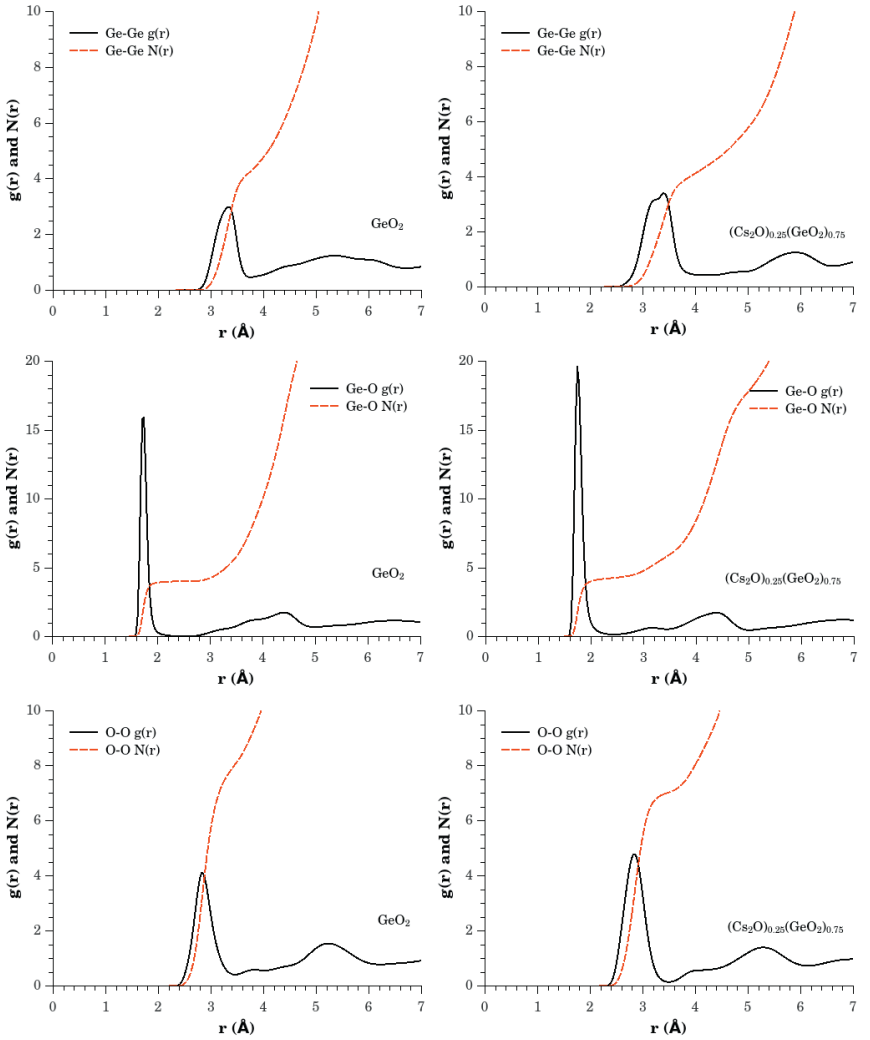

Fig. 4. The partial pair distribution functions (black solid lines) and running coordination numbers (red broken lines) for the network forming components of GeO_2 and $(Cs_2O)_{0.25}(GeO_2)_{0.75}$ glasses.

be the case for the second shell of Ge in the $(Cs_2O)_{0.25}(GeO_2)_{0.75}$ system, as $\left(N_{Ge}^{(Ge)}\right)_{2.5}^{3.8}$ remains ≈ 4, although there appears to be an enhancement in the second shell disorder, manifest by a broadening of the first peak in the $Ge-Ge$ partial pair distribution function of the ternary glass compared with GeO_2. In contrast to the behaviour of the $Si-Si$ and $Ge-Ge$ partial distribution functions, the $O-O$ terms of the ternary glasses appear to be affected to the opposite extent, in the $(SnO)_{0.282}(SiO_2)_{0.718}$ glass, there is a reduction in $\left(N_O^{(O)}\right)_{2.2}^{3.0}$ from ~ 6.0 to ~ 5.3, but little change in the definition of the shell, whilst the $(Cs_2O)_{0.25}(GeO_2)_{0.75}$ system shows a marked increase in the definition of the first $O-O$ correlation feature but with a decrease in $\left(N_O^{(O)}\right)_{2.2}^{3.4}$ from ~ 7.9 to ~ 7.0.

The investigated aluminate and gallate glass systems, $(CaO)_{0.70}(Al_2O_3)_{0.30}$ and $(PbO)_{0.67}(Ga_2O_3)_{0.33}$, serve to further illustrate the resilience of the local chemical order of the network forming elements Al and Ga, as despite the relatively large component of network modifier material, CaO and PbO, used in these systems, the well defined $Al-O$ and $Ga-O$ first shell correlations remain on average four-coordinate.

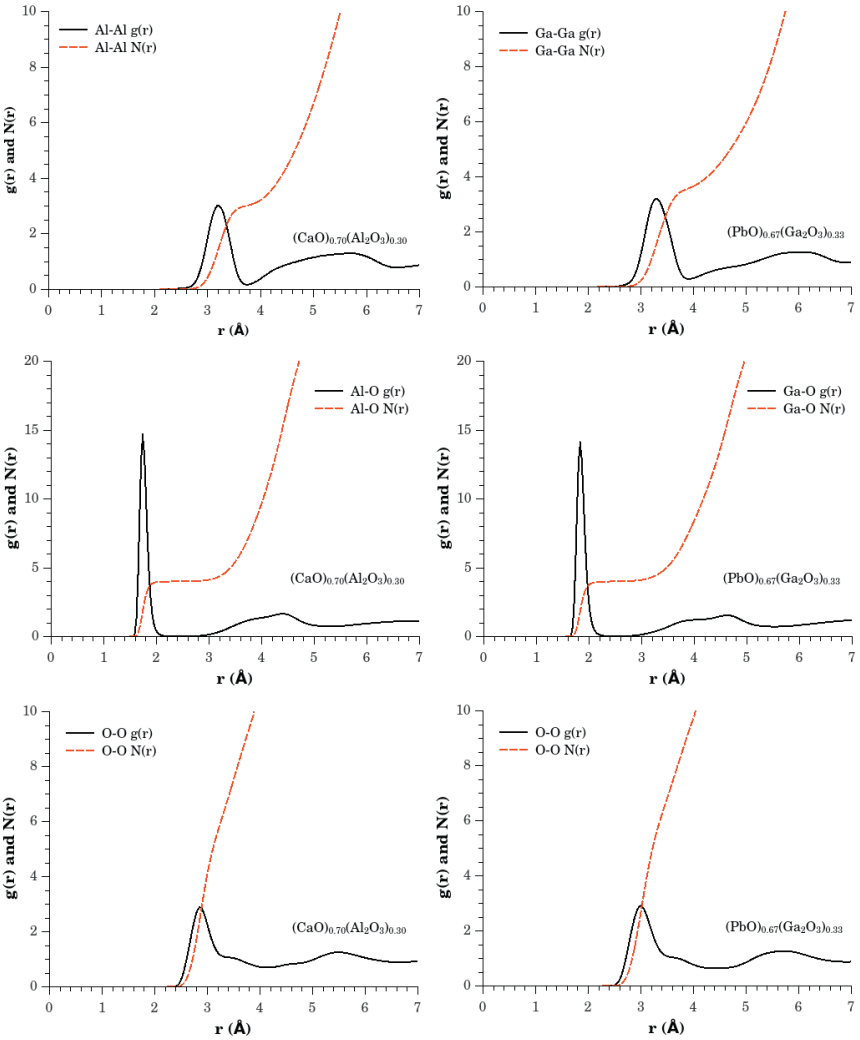

Fig. 5. The partial pair distribution functions (black solid lines) and running coordination numbers (red broken lines) for the network forming components of $(CaO)_{0.70}(Al_2O_3)_{0.30}$ and $(PbO)_{0.67}(Ga_2O_3)_{0.33}$ glasses.

4.2. Bond angle and coordination number histogams

A further advantage of performing the analysis of diffraction data using an atomistic simulation approach, is that it is a trivial matter to interrogate the models to obtain estimates of bond angle distributions and coordination number distributions. Figure 6 shows the $O-Si-O$, $O-Ge-O$, $Si-O-Si$ and $Ge-O-Ge$ bond angle distributions for the models of SiO_2, $(SnO)_{0.282}(SiO_2)_{0.718}$, GeO_2 and $(Cs_2O)_{0.25}(GeO_2)_{0.75}$. Each of these bond angle distributions has been corrected for the $\sin\theta$ dependence that would occur from sampling a random distribution of angles, Kroon and Kanters (1974). The upper panel of Figure 6 shows us that in the SiO_2 and GeO_2 glasses, the dominant network motif is tetrahedral units of SiO_4 and GeO_4 as indicated by the preferred bond angle of 109°. Interestingly this motif is largely unaffected in the $(SnO)_{0.282}(SiO_2)_{0.718}$ system, but in the $(Cs_2O)_{0.25}(GeO_2)_{0.75}$ glass, there is a marked increase in the angular disorder of the GeO_4 local units and a significant growth in linear $O-Ge-O$ linkages. Although this difference is very obvious in the bond angle distribution, it would not be as clear if one were to consider the mean $O-Si-O$ and $O-Ge-O$ values, these are $\sim$ 109° for the SiO_2, $(SnO)_{0.282}(SiO_2)_{0.718}$ and GeO_2 systems, but $\sim$ 111°

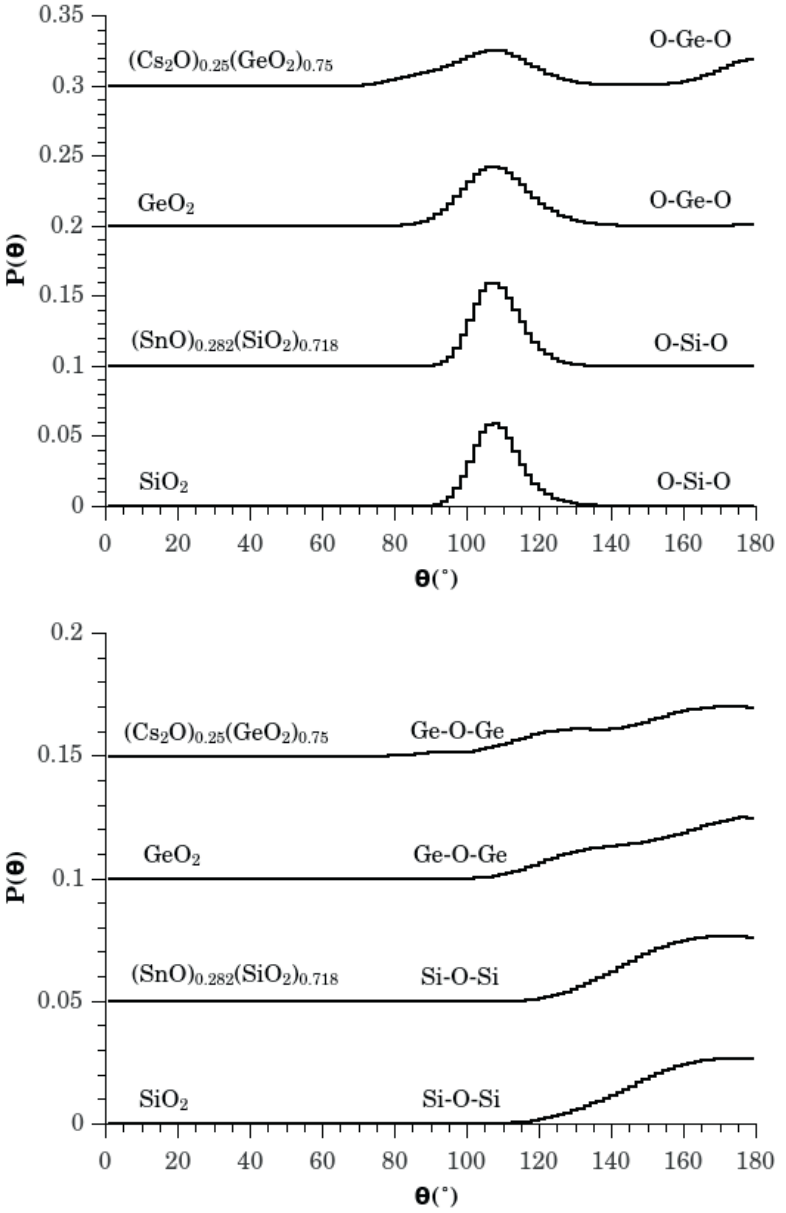

Fig. 6. $O-Si-O$ and $O-Ge-O$ bond angle distributions (upper panel) and $Si-O-Si$ and $Ge-O-Ge$ bond angle distributions (lower panel) evaluated from the EPSR models of SiO_2, $(SnO)_{0.282}(SiO_2)_{0.718}$, GeO_2 and $(Cs_2O)_{0.25}(GeO_2)_{0.75}$. $P(\theta)$ is the normalised probability distribution histogram of the specified bond angles. For clarity, in the upper panel each successive probability distribution has been offset vertically by 0.1 units, whilst in the lower panel the vertical offset is 0.05 units.

for the $(Cs_2O)_{0.25}(GeO_2)_{0.75}$ glass and hence demonstrating the value of an atomistic model for picking out subtle details of this kind.

Figure 7 shows the first shell coordination number histograms for the Si and Ge sites in the silicate and germanate glasses. This analysis allows us to probe into the aforementioned resilience of the local chemical order of the network formers in the systems we have investigated. In all four systems, there is clearly a strong preference for four-fold

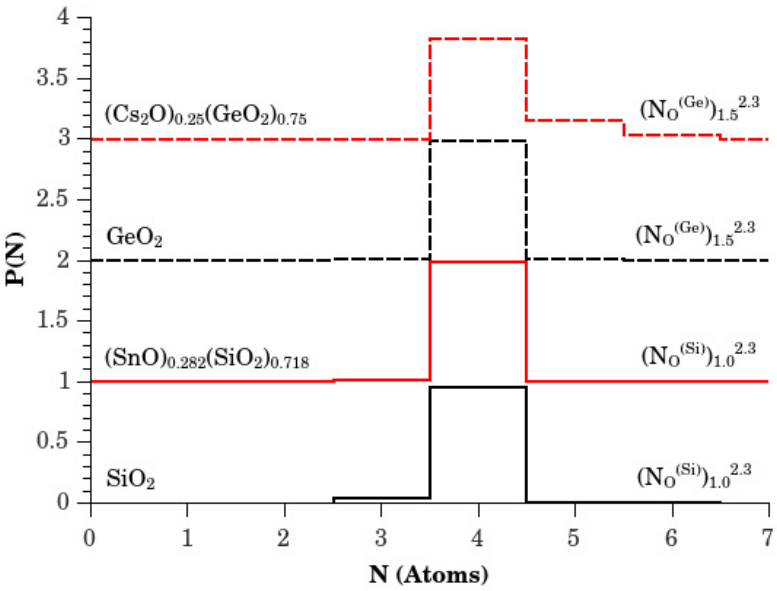

Fig. 7. First shell coordination number histograms $\left(N_O^{(Si)}\right)_{1.0}^{2.3}$ and $\left(N_O^{(Ge)}\right)_{1.5}^{2.3}$ evaluated by a site by site analysis of the EPSR models of SiO_2, $(SnO)_{0.282}(SiO_2)_{0.718}$, GeO_2 and $(Cs_2O)_{0.25}(GeO_2)_{0.75}$. $P(N)$ is the normalised probability histogram of finding N oxygen atom neighbours about the silicon or germanium atoms within the distance range indicated by the subscript and superscript numbers in the label (Ångström units). For clarity, each successive probability distribution has been offset vertically by 1.0 units.

coordination of the Si and Ge atoms by O, but in the $(Cs_2O)_{0.25}(GeO_2)_{0.75}$ we can observe that the presence of the Cs_2O network modifier produces a small, but significant increase in the number of five- and six-fold O coordinated Ge sites. This change is consistent with the observation of the increase in the number of linear $O-Ge-O$ linkages in the bond angle distribution function analysis of this glass.

4.3. Network modifier structural correlations

Having investigated the structural correlations of the networking forming elements in the glasses, it is interesting to see how the network modifiers and charge compensating species, Sn, Cs, Ca and Pb, are accommodated into the glass systems that we have investigated, Connelly et al. (2011). Figure 8 shows the partial pair distribution functions of these elements with O. The well defined peaks in $g_{xO}(r)$ and moderate plateauing in the running coordination number of the divalent network modifiers Sn, Ca and Pb, tells us that they generate well defined first coordination shells with O atoms. In contrast the much larger monovalent Cs atoms do not do this, instead they appear to occupy much more disordered first shell coordination environments.

Finally, Figure 9 shows the self correlations between the network modifier atoms as these functions are often of considerable interest to glass technologists as they can be related to issues such as ion conduction and percolation pathways, quenching of optical properties and operational aging of glassy materials.

5. Conclusions

The challenge for the structural glass scientist is frequently the extraction of the maximum amount of information from experimental data that is generally limited and incomplete. Here we have shown that physico-chemically constrained atomistic modelling, where a model is refined to reproduce available neutron or X-ray scattering data, can greatly assist in this task. It is however very important to remember that although the models permit the structure of glassy materials to be investigated in great detail, the actual constraints imposed by the experimental data may not be

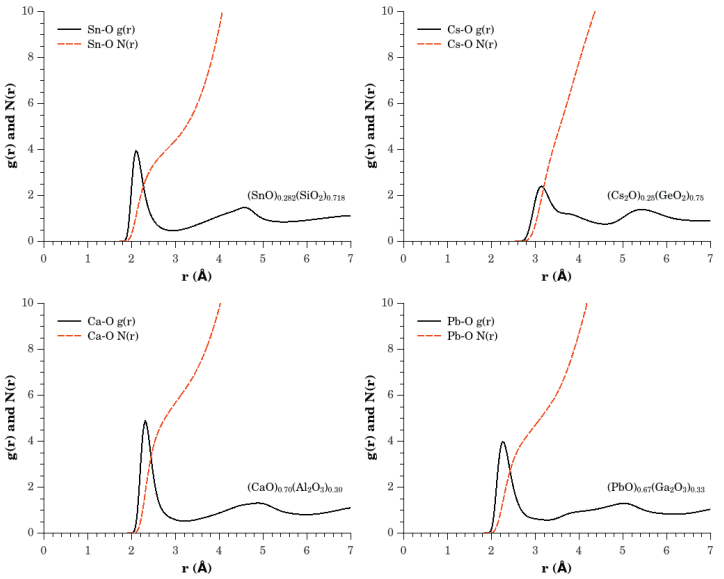

Fig. 8. The partial pair distribution functions (black solid lines) and running coordination numbers (red broken lines) for the network modifying elements in $(SnO)_{0.282}(SiO_2)_{0.718}$, $(Cs_2O)_{0.25}(GeO_2)_{0.75}$, $(CaO)_{0.70}(Al_2O_3)_{0.30}$ and $(PbO)_{0.67}(Ga_2O_3)_{0.33}$ glasses.

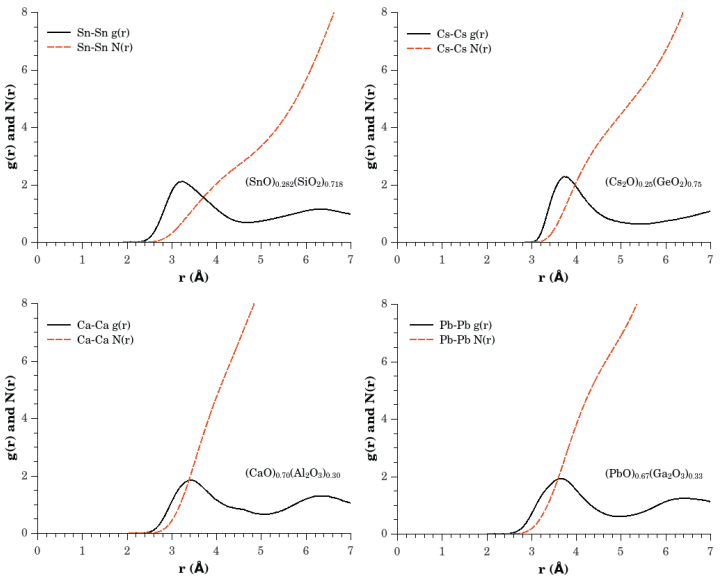

Fig. 9. The partial pair distribution functions (black solid lines) and running coordination numbers (red broken lines) for the self correlations between the network modifying elements in $(SnO)_{0.282}(SiO_2)_{0.718}$, $(Cs_2O)_{0.25}(GeO_2)_{0.75}$, $(CaO)_{0.70}(Al_2O_3)_{0.30}$ and $(PbO)_{0.67}(Ga_2O_3)_{0.33}$ glasses.

sufficient to justify any claims. In every case the investigating scientist will need to ask themselves the question as to whether it would be possible to model the data in a different way, but that is also consistent with the expected primary constraints of composition, chemical knowledge and density.

A classic example of this type of issue can be found in the *boroxol rings controversy* of liquid and glassy B_2O_3, Ferlat et al. (2009), where spectroscopic methods had for many years highlighted the importance for significant numbers of B_3O_3 ring structures in the glass network, but models based on diffraction methods and modelling had

frequently argued for only very small ring fractions, Swenson and Borjesson (1997). This issue of boroxol ring fraction is an archetypical challenge for diffraction methods as the ring configuration has no unique pair correlation function signature, instead only being uniquely characterised by higher body correlation terms.

Although we must recognise the inability of diffraction methods to be able to provide an unambiguous answer to the questions of this type, this does not prevent us from testing the competing hypotheses with methods such as EPSR. The classic case of the boroxol ring controversy has for example recently been tackled in exactly this way by Soper (2011a), to demonstrate the value of constrained modelling. Often these tests can be highly informative since if our hypotheses are found to be incompatible with the diffraction data then they can be ruled out, whilst if multiple satisfactory models can be found, then we immediately know that further discriminating evidence must be sought. An example of where complementary information of this type has been applied to the analysis of a borosilicate glass of nuclear interest can be found in this volume, Bouty (2014).

With regards to the model systems used as examples in this study, all primary conclusions about glass network structure, interatomic distances and coordination numbers were found to be consistent between the predictions of the reported EPSR models, and those obtained by conventional analysis methods, Bent et al. (1998); Grimley et al. (1990); Hannon et al. (2007, 1990); Hannon and Parker (2000); Hannon et al. (1998). This consistency highlights how reliable atomistic models can now be produced, quite simply and rapidly, that can greatly contribute to the analysis and interpretation of neutron and X-ray scattering data obtained from amorphous materials. A particular incentive for adopting the atomistic modelling approach, is that specific answers to structural questions can often be obtained very quickly and directly, without having to adopt approaches such as complex peak fitting, Bent et al. (1998) or bond-valence analyses, Hannon et al. (2007) which have their own additional uncertainties beyond those intrinsic to the diffraction data itself.

References

Allen, M.P., Tildesley, D.J., 1987. Computer Simulation of Liquids. Oxford University Press, Oxford.

Bent, J.F., Hannon, A.C., Holland, D., Karim, M.M.A., 1998. The structure of tin silicate glasses. J. Non-Cryst. Solids 232–234, 300–308.

Bouty, O., 2014. Application of the Empirical Potential Structure Refinement technique to a borosilicate glass of nuclear interest. Procedia Mat. Sci. .

Bowron, D.T., 2008a. An experimentally consistent atomistic structural model of silica glass. Mat. Sci. Eng. B 149, 166–170.

Bowron, D.T., 2008b. Experimentally consistent atomistic modeling of bulk and local structure in liquids and disordered materials by empirical potential structure refinement. Pure Appl. Chem. 6, 1211–1227.

Connelly, A.J., Hyatt, N.C., Travis, K.P., Hand, R.J., Maddrell, E.R., 2011. Predicting the preference for charge compensation in silicate glasses. Phys. Chem. Glass. 52, 64–67.

Cusack, N.E., 1987. The Physics of Structurally Disordered Matter: An Introduction. Adam Hilger, Bristol.

Enderby, J.E., North, D.E., Egelstaff, P.A., 1966. Partial structure factors of liquid Cu-Sn. Phil. Mag. 14, 961–970.

Ferlat, G., Charpentier, T., Seitsonen, A.P., Takada, A., Lazzeri, M., Cormier, L., Calas, G., Mauri, F., 2009. Boroxol rings in liquid and vitreous B2O3 from first principles. Phys. Rev. Lett. 101, 065504.

Fischer, H.E., Barnes, A.C., Salmon, P.S., 2006. Neutron and X-ray diffraction studies of liquids and glasses. Rep. Prog. Phys. 69, 233–299.

Fuoss, P.H., Eisenberger, P., Warburton, W.K., Bienenstock, A., 1981. Application of Differential Anomalous X-Ray Scattering to Structural Studies of Amorphous Materials. Phy. Rev. Lett. 46, 1537–1540.

Grimley, D.I., Wright, A.C., Sinclair, R.N., 1990. Neutron scattering from vitreous silica iv. Time-of-flight diffraction. J. Non-Cryst. Solids 119, 49–64.

Hannon, A.C., Di Martino, D., Santos, L.F., Almeida, R.M., 2007. Ge-O coordination in cesium germanate glasses. J. Phys. Chem. B 111, 3342–3354.

Hannon, A.C., Howells, W.S., Soper, A.K., 1990. ATLAS - A suite of programs for the analysis of time-of-flight neutron diffraction data from liquid and amorphous samples. IOP Conf. Series 107, 193–211.

Hannon, A.C., Parker, J.M., 2000. The structure of aluminate glasses by neutron diffraction. J. Non-Cryst. Solids 274, 102–109.

Hannon, A.C., Parker, J.M., Vessal, B., 1998. Neutron diffraction analysis of the atomic short range order in lead gallate glasses. J. Non-Cryst. Solids 232, 51–58.

Keen, D.A., 2001. A comparison of various commonly used correlation functions for describing total scattering. J. Appl. Cryst. 34, 172–177.

Kroon, J., Kanters, J.A., 1974. Non-linearity of hydrogen bonds in molecular crystals. Nature 248, 667–669.

Lovesey, S.W., 1984. Theory of Neutron Scattering from Condensed Matter. Volume 1: Nuclear Scattering. Oxford University Press, Oxford.

Sears, V.F., 1992. Neutron scattering lengths and cross sections. Neutron News 3, 29–37.

Soper, A.K., 1996. Empirical potential Monte Carlo simultion of fluid structure. Chem. Phys. 202, 295–306.

Soper, A.K., 2005. Partial structure factors from disordered materials diffraction data: An approach using empirical potential structure refinement. Phys. Rev. B 72, 104204.

Soper, A.K., 2011a. Boroxyl rings from diffractions data on vitreous boron trioxide. J. Phys. Condens. Matter 23, 365402.

Soper, A.K., 2011b. Empirical Potential Structure Refinement - EPSRshell: a user's guide. Version 18 - May 2011. volume RAL-TR-2011-012. Rutherford Appleton Laboratory Technical Report, Oxfordshire, UK.

Soper, A.K., 2011c. GudrunN and GudrunX: programs for correcting raw neutron and X-ray diffraction data to differential scattering cross section. volume RAL-TR-2011-013. Rutherford Appleton Laboratory Technical Report, Oxfordshire, UK.

Swenson, J., Borjesson, L., 1997. Fraction of boroxol rings in vitreous boron trioxide. Phys. Rev. B 55, 11138–11143.

Waasmaier, D., Kirfel, A., 1995. New analytical scattering factor functions for free atoms and ions. Acta. Cryst. A51, 416–431.

Zallen, R., 1983. The Physics of Amorphous Solids. Wiley-VCH, Weinheim.